# Average Capacity Evaluation Performance for Transdermal Optical Wireless Communications under the Effect of Pointing Error

https://doi.org/10.3991/ijoe.v18i13.33653

Omar M. Hasan(✉)
Department of Communication Engineering, Princess Sumaya University for Technology, Amman, Jordan
ohasan@psut.edu.jo

**Abstract—**In this paper, we investigate the performance of average capacity of transdermal wireless optical communication system under the effect of pointing error and skin attenuation. The channel statistical model is assumed to be the product of a stochastic process due to pointing error, and a constant channel gain caused by the skin attenuation. Furthermore, the transdermal optical wireless system employs intensity modulation direct detection with on-off signaling (IMDD/OOK). The pointing error stochastic process model considers the zero boresight case. We derive novel closed form expression for the average capacity which takes into account the effect of geometric spreading due to pointing error, and the transdermal channel pathloss. Numerical results for the average capacity are provided as a function of the received signal-to-noise ratio, and the results are shown for different pointing error severity levels, and transdermal pathloss due to skin attenuation.

**Keywords—**average capacity, transdermal wireless optical (TWO) system, channel intensity modulation direct detection with on-off keying (IMDD/OOK), zero boresight

## 1 Introduction

Recent advances in implanted medical devices (IMDs) has embarked many biomedical applications such as health monitoring, neural recording, prostheses and telemetry with medical implants. However, IMD applications require robust wireless communication systems capable of providing high speed rates for the stimulated signals and exchange of data within these devices. It is well known that optical wireless communications (OWCs) can be a suitable technology [1–6], to meet IMD demand for high speed data rate systems and its immunity to interference from nearby radio frequency medical devices. In fact, OWC technology can offer 1–2 Gb/sec systems, and can be easily deployed. In addition, OWC technology is low power, cost effective, and requires no licensing for deployment, and hence can be a suitable alternative for radio frequency communications currently used in AMD applications.

The use of OWC technology to provide the communication base for the IMD defines what is known by Transdermal Optical Wireless (TOW) communication [1–5].

The feasibility and the suitability of transdermal optical wireless links (TOLs) have been experimentally validated by many researchers [7–13]. The work by [7–9], was mainly performed to study the optical properties of the human skin and subcutaneous tissues. In [7], the author has conducted a vitro experiment aiming at studying the optical properties of human skin. The experiment was conducted by taking samples of skin specimens of three different individuals in the spectral range of 400–1800 nm. The author provided measured results for the diffuse reflectance and transmittance of the three different tissues. On the other hand, the authors in [10–13], have validated the feasibility of the OWCs for the transcutaneous links. In vivo tests, the author in [13], reported that the optical wireless link is capable of transmitting data at a speed of 100 Mbps with a bit error rate (BER) of, $2.10^{-7}$ consuming only 2.1 mW of electrical power.

There are two main draw backs in TOLs. The first being the transdermal pathloss [11–15], due to signal attenuation caused by the multilayered skin structure. Signal attenuation occurs since the information bearing light signal propagation through the skin is reflected, scattered and absorbed by multilayered skin structure. In fact, the multilayered skin structure can also limit the propagation depth of the information-bearing light signal into the tissue by several centimeters [10], [15–16]. The second drawback of TOLs is the pointing error due to the random misalignment between the transmitter and the receiver. In fact, pointing error not only caused by misalignment between the transmitter and the receiver, but it is also caused by the relative motion between the transmitter and the receiver due to the nature activity of biological function induced in the skin tissues [15]. Accurate pointing error process is modeled by nonzero stochastic model which is composed of two components known as the boresight and jitter. The boresight component represents a fixed displacement between the beam and the detector center, while the jitter is the beam center random offset at the detector plane [5], [15], [17–21].

In TOWs, the direct model and modulator retroreflective (MRR) are usually used to configure the transdermal optical link [19–21]. In the direct configuration, the external unit acts as the transmitter in order to convey the external modulated stimulated signal through the skin to the implanted unit to produce the proper stimulation. In MRR, the external laser transmitter emits the laser signal through the skin toward the retro-reflector (RR) which is located in the implanted device, then RR unit modulates the incoming laser signal and reflected it back to the out of body receiver to produce the proper stimulation. In the MRR configuration, since both the transmitter and receiver terminals are outside of body, the light signal has to propagate through the skin channel twice, thus, causing more induced channel attenuation. However, MRR technology is more robust in terms of its ease of deployment and longer battery life time of the implanted unit, since most of the signal processing takes place at the out-of-body transceiver.

In [15], signal quality assessment for direct configured TOW under the effect of pointing was studies and analyzed. The authors provided results for average SNR for different dermis skin thickness, wavelengths ranging from 400 *nm* to 1800 *nm*, pointing error variance and system parameters. Outage performance for TOL with pointing has been studied by [20]. The authors provided closed form expression for evaluating the outage probability, which takes into account the effect of pointing error, characteristics of optical unit and channel particularities. Their results reveal that pointing errors drastically affect the reliability and effectiveness of the link and should be taken into consideration when designing a transdermal OWC link. Finally, average BER results for MRR TOW system with spatial diversity were provided by [21], under the effect of pointing error. The authors provided novel analytical mathematical expression for the BER, which takes into account the effect of NZB pointing error, channel induced skin attenuation and average SNR. The authors reported that significant outage improvement can be attained when using spatial diversity.

In this paper, we will investigate and analyze the performance of direct configured TOW system under the effect of pointing error. In this context, we will derive closed form expression for average capacity, which takes into account the effect pointing error severity, skin induced attenuation and system parameters.

The paper is organized as follows. In Section II, we provide description and analysis for the system under study. Analysis in this section is developed for ZB pointing error. In section III, we derive a closed form solution for the system average capacity. In the following section IV, we provide numerical results for system average capacity as a function of average SNR, for different levels of pointing error severity and skin thickness. In section V, we summarize our work and provide our comments and conclusions.

## 2 System and channel model

In the analysis to follow, we assume perfect skin channel state information (CSI) and direct transdermal optical wireless link configuration as shown in Figure 1. In addition, we assume transdermal optical wireless communications system deploying intensity modulated direct detection with on-off keying modulation IMDD/OOK. The proposed TOW system consist of an out-of-body unit which emits stimulation light messages to the implanted device (in-body unit) through the skin. The information-bearing light signal propagates through the skin, and once it is arrive at the receiver, the light intensity is directly detected and demodulated to recover the information data to invoke the proper stimuli. The baseband equivalent received signal at the photo detector is given by [20]

$$y = \eta \cdot h x + n \tag{1}$$

Where $\eta$ is the photodiode's efficiency, and $x \in \{0,1\}$, is the OOK data information signal, while $n$ is zero mean Gaussian process with variance $\sigma_n^2$, and power spectral density $N_0/2$ watts/Hz.

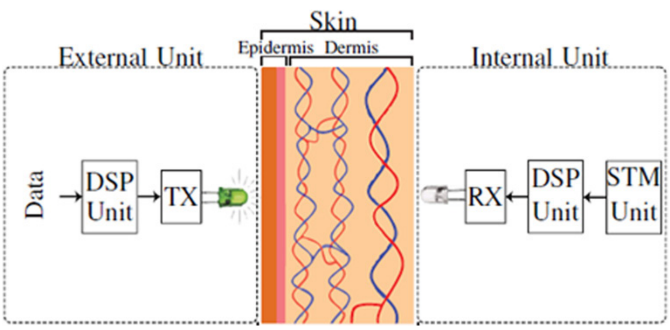


**Fig. 1.** System model [20]

In eq. (1), $h$ is the skin channel state and has the form [20]

$$h = h_l \cdot h_p \tag{2}$$

Where $h_l$ is a deterministic term representing the transdermal channel path loss due to skin attenuation, and $h_p$ is a stochastic process representing the pointing error process between the external unit and internal unit. The determinstic term can be represented as [15]

$$h_l = \exp(-0.5\alpha(\lambda) \cdot \delta) \tag{3}$$

The parameter $\delta$ is the dermis thickness and $\lambda$ being the operating wavelength in "*nm*". The term $\alpha(\lambda)$ represents the skin attenuation coefficient and can be evaluated for $\lambda = 400$ *nm* $\lambda = 1800$ *nm* using

$$\alpha(\lambda) = \sum_{i=1}^{8} a_i \cdot \exp\left[-\left(\frac{\lambda - b_i}{c_i}\right)^2\right] \tag{4}$$

The coefficients $a_i$, $b_i$, and $c_i$, can be evaluated using [15], as shown below in Table 1.

**Table 1.** Coefficients $a_i$, $b_i$, and $c_i$ values [15]

| ***i*** | $a_i$ | $b_i$ | $c_i$ |
|---|---|---|---|
| 1 | 10 | 0.35 | 0.065 |
| 2 | 4.5 | 0.42 | 0.25 |
| 3 | 13.478 | −1.50 | 50.12 |
| 4 | 14.7 | 1442 | 49.35 |
| 5 | 7.435 | 1499 | 75.88 |
| 6 | 48 | 3322 | 1033 |
| 7 | 594.1 | −183 | 285.9 |
| 8 | 11.47 | −618.5 | 1054 |

The stochastic skin channel term $h_p$ can highly degrade the performance of the TOLs, which represents fraction of the collected power due to geometric spread with radial displacement $r$ from the origin of the detector [5], causing an offset between the incident beam footprint and the detector aperture measured on the plane of the detector. The channel random variable $h_p$ has a probability density function [5]

$$h_p \approx A_o \exp\left(-\frac{2r^2}{w_{eq}^2}\right) \tag{5}$$

Where $A_o$ is the fraction of the collected power at $r = 0$, evaluated using

$$A_o = [\text{erf}(v)]^2 \tag{6}$$

The notation erf (∗) is the error function, an *v* can be evaluated using

$$v = \frac{\sqrt{A}}{\sqrt{2}\omega_\delta} \tag{7}$$

The parameter A is the photodiode effective area given by $A = \pi \cdot a^2$, where *a* represents the radius of the circular receiving aperture, and $\omega_\delta$ is the beam waste (radius calculated at $e^{-2}$) on the RX plane at distance δ from the transmitter, and can be obtained using

$$\omega_\delta = \delta \cdot \tan(\theta/2) \tag{8}$$

Where $\theta$ represents the divergence angle of the transmitted beam The parameter $\omega_\delta$ ia the beam waste (calculated at $e^{-2}$) on the receiver plane at distance δ from the transmitter. The equivalent beam width $w_{zq}$ can be evaluated using

$$\omega_{zq}^2 = \omega_\delta^2 \frac{\sqrt{\pi}\,\mathrm{erf}\,(v)}{2v\exp(-v^2)} \tag{9}$$

As assumed by [5], the radial displacement *r* at the receiver is modeled by a Rayleigh distribution as

$$f_r(r) = \frac{r}{\sigma_s^2}\exp\left(-\frac{r^2}{2\sigma_s{}^2}\right),\ r > 0 \tag{10}$$

The parameter $\sigma_s^2$ is the jitter variance at the receiver. As a result, it was shown by [5], the channel random term *hp* can be obtained as

$$f_{hp}(h_p) = \frac{\xi}{A_o^\xi} h_p{}^{\xi-1}, \qquad 0 \le x \le A_o \tag{11}$$

Where $\xi$ is the ratio between the equivalent beam radius at the receiver and the pointing error displacement standard deviation at the receiver given by

$$\xi = \frac{w_{zq}}{2 \cdot \sigma_s^2} \tag{12}$$

By using eqs. (2) and (11), the channel pdf can be found as

$$f_h(h) = \frac{\xi}{A_o^\xi h_l^\xi} h^{\xi-1}, \qquad 0 \le x \le A_o h_l \tag{13}$$

## 3 Average capacity analysis

In the analysis to follow, we assume perfect skin channel state information (CSI). Furthermore, by assuming an intensity modulation and direct detection (IM/DD) transdermal optical wireless link with zero-mean and variance $\sigma^2 = N_o/2$, where $N_0$ is the noise power spectral density.

To evaluate the average channel capacity, we start by the well-known channel capacity equation

$$C = B \cdot log_2[1+\gamma] \tag{14}$$

Where $B$ is the bandwidth, and $\gamma$ is the signal-to-noise ratio. Since the TOL contains the random term $h_p$, then the signal-to-noise ratio $\gamma$ is random and assumed to be constant over at least a couple of symbol intervals, as a result, the average capacity $\overline{C}$ is can be evaluated using

$$\overline{C} = \int_0^\infty B \cdot log_2[1+\gamma(h) \cdot f_h(h)\, dh \tag{15}$$

Here $\gamma(h)$ is the received instantaneous signal-to-noise ratio, and $f_h(h)$ is the probability density function (pdf) of $h$ given by eq. (13). For the case study, for intensity modulation and direct detection (IM/DD), the received instantaneous signal-to-noise ratio $\gamma(h)$ can be expresses as [20]

$$\gamma(h) = \frac{\eta^2 \exp\{-\alpha(\lambda)\cdot\delta\} h^2 \cdot P_s}{\sigma^2} \tag{16}$$

Where $P_S$ is the average optical power of the transmitted light signal, while the parameters $\alpha(\lambda)$, $\delta$, $h$ as previously defined in section II. By inserting the noise variance $\sigma^2 = N_o/2$ in (16), $\gamma(h)$ can be written as

$$\gamma(h) = \frac{\eta^2 \exp\{-\alpha(\lambda)\cdot\delta\} h^2 \cdot \overline{P}_s}{N_0} \tag{17}$$

The parameter $\overline{P}_s$ is the transmitted signal power spectral density. As can be seen from (17), the statistics of the instantaneous SNR $\gamma$, depends on the statistics of the channel random term $h^2$. The average value of $\gamma(h)$ is evaluated as

$$E[\gamma(h)] = \overline{\gamma} = E\left[\frac{\eta^2 \exp\{-\alpha(\lambda)\cdot\delta\}\cdot h^2 \cdot \overline{P}_s}{N_0}\right] \tag{18}$$

The notation $E[*]$ denotes expectation. So, $\overline{\gamma}$ is evaluated using

$$\overline{\gamma} = \frac{\eta^2 \exp\{-\alpha(\lambda)\cdot\delta\}\cdot \overline{P}_s}{N_0} E[h^2] \tag{19}$$

Where $E[h^2]$ is evaluated as

$$E[h^2] = \int_0^{A_o} h^2 \frac{\xi}{A_o^{\xi} h_l^{\xi}} h^{\xi-1}\, dh = \frac{\xi \cdot (A_o h_l)^2}{(\xi+2)} \tag{20}$$

Thus,

$$\bar{\gamma} = \frac{\xi \cdot (A_o h_l)^2 \cdot \eta^2 \exp\{-\alpha(\lambda)\cdot\delta\} \cdot \bar{P}_s}{(\xi+2)\cdot N_0} \tag{21}$$

By inserting eqs. (11) and (16) into eq. (14), the average capacity can be written as

$$\bar{C} = \int_0^{A_0 h_l} B \cdot log_2[1 + k \cdot h^2) \cdot \frac{\xi}{(A_o h_l)^{\xi}} h^{\xi-1} dh \tag{22}$$

Where the constant $k$ is evaluated using

$$k = \frac{\eta^2 \exp\{-\alpha(\lambda)\cdot\delta\}\cdot \bar{P}_s}{N_0} \tag{23}$$

By letting $x = k \cdot h^2$, and going through some mathematical manipulations, the average capacity can be written as

$$\bar{C} = \frac{\xi B}{2k^{\xi/2}(A_o h_l)^{\xi}} \int_0^{k(A_o h_l)^2} log_2[1+x)\cdot(x)^{\frac{\xi}{2}-1} dx \tag{24}$$

By using the identity $log_a(z) = \ln(z)/\ln(2)$, where ln, is the natural logarithmic function. As a result, eq. (24) can be written as

$$\bar{C} = \frac{\xi B}{2\ln(2)\cdot k^{\xi/2}(A_o h_l)^{\xi}} \int_0^{k(A_o h_l)^2} \ln[1+x)\cdot(x)^{\frac{\xi}{2}-1} dx \tag{25}$$

By using [22, 01.05.26.0002.01], the average $\bar{C}$ can be written in terms of Meijer's G function as

$$\bar{C} = \frac{\xi B}{2\cdot\ln(2)\cdot k^{\xi/2}(A_o h_l)^{\xi}} \int_0^{k(A_o h_l)^2} G_{2,2}^{1,2}\left[x \left| \begin{matrix} 1,1 \\ 1,0 \end{matrix} \right.\right]\cdot(x)^{\frac{\xi}{2}-1} dx \tag{26}$$

Using [23, eq. (26)], the average capacity can be evaluated as

$$\bar{C} = \frac{\xi B}{2\cdot\ln(2)\cdot k^{\xi/2}(A_o h_l)^{\xi}} (k(A_o h_l)^2)^{\frac{\xi}{2}} G_{3,3}^{1,3}\left[k(A_o h_l)^2 \left| \begin{matrix} 1,1,1-\frac{\xi}{2} \\ 1,-\frac{\xi}{2}.0 \end{matrix} \right.\right] \tag{27}$$

Finally, the average capacity can be written in terms of the average SNR as

$$\bar{C}/B = \frac{\xi}{2 \cdot \ln(2)} \cdot G_{3,3}^{1,3}\left[\frac{(\xi+2)}{\xi}\bar{\gamma}\left|\begin{matrix}1,1,1-\frac{\xi}{2} \\ 1,-\frac{\xi}{2}.0\end{matrix}\right.\right] \tag{28}$$

## 4 Numerical results

In this section, we assume direct transdermal optical wireless communications system deploying intensity modulated direct detection with on-off keying modulation IMDD/OOK. Unless otherwise stated, Table 2, shows the parameters used in this section.

**Table 2.** System and channel used parameters

| Symbol | Referenced Item | Value |
|---|---|---|
| $\eta$ | Responsivity | 0.80 |
| $\lambda$ | Operating wavelength | 1500 nm |
| $\alpha(\lambda)$ | Skin attenuation | 1.8 |
| $A$ | Photodiode effective area | 1 $mm^2$ |
| $N_o$ | Noise PSD | $(1.3pA/\sqrt{Hz})^2$ |
| $P_x$ | Signal PSD | 0.1 mw/Hz |
| $\delta$ | Skin thickness | 9 mm |
| $\theta$ | Divergence angle | 20° |

Figure 2, shows results for average capacity versus average $\bar{\gamma}$, for $\zeta$ = 0.1, 0.25, 0.50, 0.75, 1.0. As we can see from the figure, for any given value of SNR, as $\zeta$ increases, better average capacity performance can be achieved. This is expected since an increase in $\zeta$, leads to a decrease in the pointing error displacement standard deviation at the receiver. In addition, this implies a larger equivalent beam radius at the receiver as depicted by eq. (12).

Figure 3, shows results for the average capacity for different values of the divergence angle, as a function of average SNR values. In addition, it was assumed that pointing error standard deviation $\sigma_S$ = 1.442, the wavelength $\lambda$ = 850 nm, and the detector radius $\alpha$ = 0.5 mm, while the skin thickness was set to $\delta$ = 10 mm. As can be seen form the figure, for any given value of average, as the divergence angle increases, the average capacity increases too.

Figure 4, depicts results for the average capacity as a function of average SNR, for different values of skin thickness and pointing error standard deviation. It was also assumed that $\lambda$ = 1000 nm. As we can see from the figure, for any given value of $\sigma_S$, as the skin thickness increases, the average capacity is degraded due to an increase in the skin attenuation.

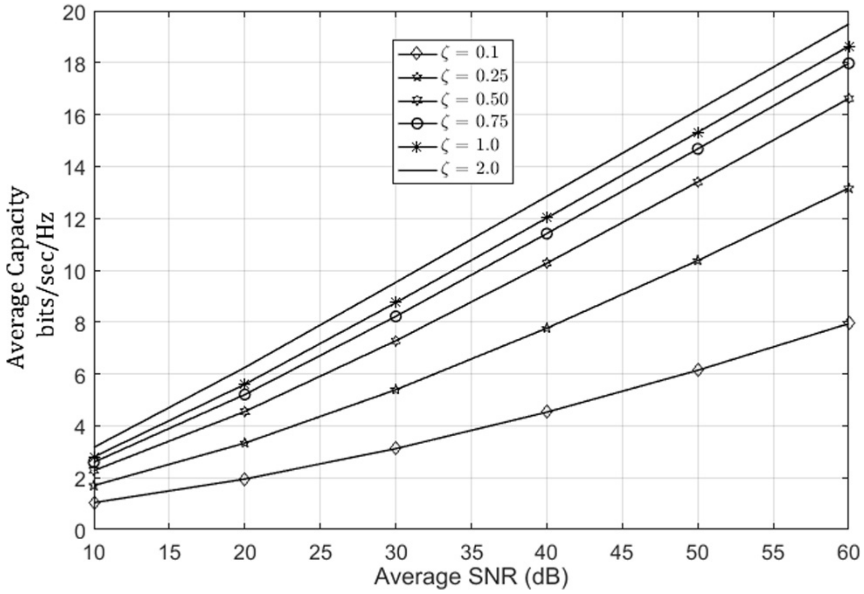


**Fig. 2.** Average capacity versus average electrical SNR for $\lambda$ = 1500 nm

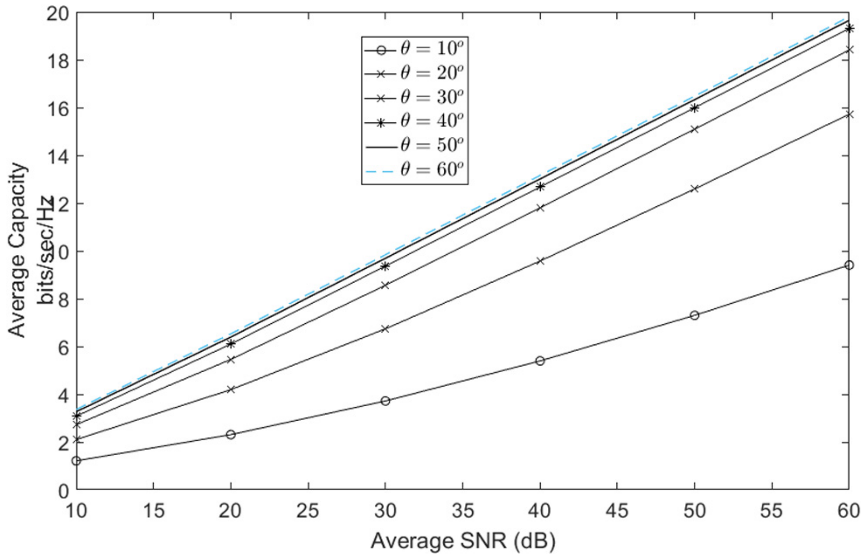


**Fig. 3.** Average capacity versus divergence angle

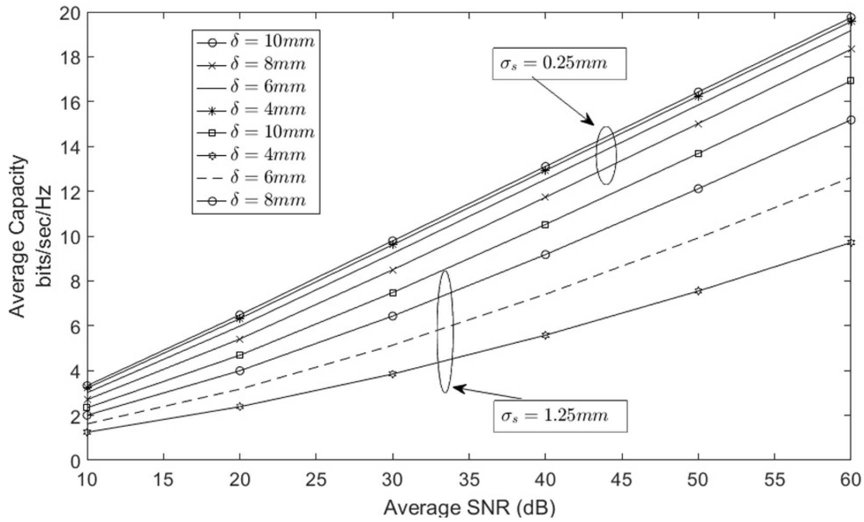


**Fig. 4.** Average capacity for different values of skin thickness and jitter variance

## 5 Conclusion

In this paper, we have analyzed the performance of transdermal optical wireless communications system deploying intensity modulated direct detection with on-off keying modulation IMDD/OOK. The proposed TOW system consist of an out-of-body unit which emits stimulation light messages to the implanted device (in-body unit) through the skin. We have derived novel closed form expression for average capacity which contains the system and channel parameters. The derived expression allows for evaluating the performance of average capacity which was useful in the evaluation and reasoning for system performance in terms of the system and channel parameter. It was also demonstrated that, in evaluating the TOW system performance, there are many parameters that should be taken into account in order to optimize its performance, the wavelength, the signal power, and TOW system configuration.

## 6 Acknowledgment

This research was supported by Princess Sumaya University for Technology under agreement 7(31) - 2019/2020.

## 7 References

[1] Gyan Deep Verma, and Aashish Mathur, "Performance improvement of FSO communication systems using hybrid-ARQ protocols," Applied optics, vol. 60, no. 19, pp. 5553–5563, 2021. https://doi.org/10.1364/AO.424687

[2] Mehtab Singh, and Jyoteesh Malhotra, "Long-reach high-capacity hybrid MDM-OFDM-FSO transmission link under the effect of atmospheric turbulence," Wireless pesonal Commn. 107, vol. 67, no. 4, pp. 1549–1571, 2019. https://doi.org/10.1007/s11277-019-06345-7
[3] M. Kashani, M. Uysal, and M. Kavehrad, "A novel statistical model for turbulence-induced fading in free-space optical systems," in Proceedings of the 15th International Conference on Transparent Optical Networks (ICTON), pp. 1–5, June 2013. https://doi.org/10.1109/ICTON.2013.6602795
[4] Omar M. Hasan, "Bit Error and Outage Rate Results for Non-Zero Turbulence Cells Over Gamma-Gamma Free Space Optical Wireless Channel," *J. Opt. Commun*. Vol. 34, no. 4, pp. 385–391, 2013. https://doi.org/10.1515/joc-2013-0051
[5] Ahmed A. Farid, and Steve Hranilovic, "Outage capacity optimization for free-space optical links with pointing errors," Journal of Lightwave Technology, vol. 25, no. 7, pp. 1702–1710, 2007. https://doi.org/10.1109/JLT.2007.899174
[6] C. Simatis, H. E. Nistazakis, and G. S. Tombras, "Performance and reliability investigation of free space optical communication systems over Gamma Gamma Modeled channels," http://www.atm.com
[7] Eric K. Chan, Brian Sorg, Dmitry Protsenko, Michael O'Neil, Massoud Motamedi, and Ashley J. Welch, "Effects of Compression on Soft Tissue Optical Properties," IEEE Journal of Selected Topics in Quantum Electronics, vol. 2, no. 4, pp. 943–950, 2012. https://doi.org/10.1109/2944.577320
[8] A. N. Bashkatov, E. A. Genina, and V. V. Tuchin, "Optical properties of skin, subcutaneous, and muscle tissues: a review," Journal of Innovative Optical Health Sciences, vol. 4, no. 01, pp. 9–38, Jan. 2011. https://doi.org/10.1142/S1793545811001319
[9] A. Bashkatov, E. Genina, V. Kochubey, and V. Tuchin, "Optical properties of human skin, subcutaneous and mucous tissues in the wavelength range from 400 to 2000 nm," J. Phys. D: Appl. Phys., vol. 38, no. 15, p. 2543, July 2005. https://doi.org/10.1088/0022-3727/38/15/004
[10] J. L. Abita, and W. Schneider, "Transdermal optical communications," Johns Hopkins Apl Technical Digest, vol. 25, no. 3, p. 261–268, 2004.
[11] Y. Gil, N. Rotter, and S. Arnon, "Feasibility of retroreflective trans dermal optical wireless communication," Appl Opt, vol. 51, no. 18, pp. 4232– 4239, Jun. 2012. https://doi.org/10.1364/AO.51.004232
[12] T. Liu, J. Anders, and M. Ortmanns, "System level model for transcutaneous optical telemetric link," in IEEE International Symposium on Circuits and Systems (ISCAS), pp. 865–868, May 2013.
[13] T. Liu, U. Bihr, J. Becker, J. Anders, and M. Ortmanns, "In vivo verification of a 100 mbps transcutaneous optical telemetric link," in IEEE Biomedical Circuits and Systems Conference (BioCAS), pp. 580–583, Oct. 2014. https://doi.org/10.1109/BioCAS.2014.6981792
[14] D. M. Ackermann, B. Smith, K. L. Kilgore, and P. H. Peckham, Design of a high speed transcutaneous optical telemetry link. In Proceedings of the 2006 International Conference of the IEEE Engineering in Medicine and Biology Society, New York, NY, USA, 30 August–3 September 2006; IEEE: Piscataway, NJ, USA, 2006; pp. 2932–2935. https://doi.org/10.1109/IEMBS.2006.260398
[15] S. Trevlakis, A. Boulogeorgos, and G. Karagiannidis, "Signal quality assessment for transdermal optical wireless communications under pointing errors," Technologies vol. 6. no, 109, 2018. https://doi.org/10.3390/technologies6040109
[16] T. Liu, U. Bihr, S. M. Anis, and M. Ortmanns, Optical transcutaneous link for low power, high data rate telemetry. In Proceedings of the 2012 Annual International Conference of the IEEE Engineering in Medicine and Biology Society (EMBC), San Diego, CA, USA, 28 August–1 September 2012; IEEE: Piscataway, NJ, USA, 2012; pp. 3535–3538.

[17] R. Boluda-Ruiz, A. Garcia-Zambrana, B. Castillo-Vazquez, and C. Castillo-Vazquez, "Impact of nonzeroboresight pointing error on ergodic capacity of MIMO FSO communication systems," Opt. Express vol. 24, no. 4, pp. 3513–3534, 2016. https://doi.org/10.1364/OE.24.003513
[18] G. K. Varotsos, H. E. Nistazakis, K. Aidinis, F. Jaber, and K. K. Rahman, "Transdermal optical wireless links with multiple receivers in the presence of skin-induced attenuation and pointing errors," Computation vol. 7, no. 3, p. 33. 2019. https://doi.org/10.3390/computation7030033
[19] G. K. Varotsos, H. E. Nistazakis, W. Gappmair, H. G. Sandalidis, and G. S. Tombras, "SIMO subcarrier PSK FSO links with phase noise and non-zero boresight pointing errors over turbulence channels," IET Commun. vol. 13, no. 7, pp. 831–836, 2019. https://doi.org/10.1049/iet-com.2018.5608
[20] S. E. Trevlakis, A. A. Boulogeorgos, and G. K. Karagiannidis, "Outage Performance of transdermal optical wireless links in the presence of pointing errors," 2018 IEEE 19th International Workshop on Signal Processing Advances in Wireless Communications (SPAWC), 2018, pp. 1–5. https://doi.org/10.1109/SPAWC.2018.8445766
[21] G. Varotsos, H. Nistazakis, K. Aidinid, F. Jaber, M. Nasor, and K. k. Rahman, "Error performanc estimation of modulated retroreflective transdermal optical wireless links with diversity under generalized pointing error," Telecom, Vol. 2, No. 2, pp. 167–180, 2021. https://doi.org/10.3390/telecom2020011
[22] The wolfram Function site, http://functions.wolfram.com.
[23] V. S. Adamchick, and O. I Mariachev, "The algorithm for calculating integrals of hypergeometric type and its realization in reduce system," in Proc. International Conf. on symbolic and algebraic computation, Tokyo, Japan, 1990, pp. 212–224. https://doi.org/10.1145/96877.96930
[24] H. G. Sandalidis, T. A. Tsiftsis, G. K. Karagiannidis, and M. Uysal, "BER performance of FSO links over strong atmospheric turbulence channels with pointing errors," in IEEE Communications Letters, vol. 12, no. 1, pp. 44–46, January 2008. https://doi.org/10.1109/LCOMM.2008.071408
[25] S. Arnon, "Effects of atmospheric turbulence and building sway on optical wireless-communication systems," Opt. Lett., vol. 28, no. 2, pp. 129–131, Jan. 2003. https://doi.org/10.1364/OL.28.000129
[26] Hessa AlQuwaiee, Imran Shafique Ansari, and Mohamed-Slim Alouini, "On the performance of free-space optical wireless communication systems over double generalized gamma fading channels," The fourth international conference of communcations an networking (Com Net), Hammamet, Tunisia, 19–22, March 2014, pp. https://doi.org/10.1109/ComNet.2014.6840927
[27] Hector E. Nistazakes, Andrew D. Tsigopoulos, Michalis P. Hanias, Christos D. Psychogios, Dimitris Maronos, Costas Aidinis, and George S. Tombras, "Estimation of outage capacity for free space optical links over I-K and K turbulence channels," Radio Engineering, vol. 20, no. 2, June 2011, pp. 493–498.
[28] H. E. Nistazakisa, V. D. Assimakopoulosb, and G. S. Tombrasa, "Performance estimation of free space optical links over negative exponential atmospheric turbulence channels," Inter. J. for Light & Electron Optics," vol. 122, no. 24, pp. 2191–2194, 2011. https://doi.org/10.1016/j.ijleo.2011.01.013
[29] Nestor D. Chatzidiamantis, Harilaos G. Sandalidis, George K. Karagiannidis, Stavros A. Kotsopoulos, and Michail Mattaiou, "New results on turbulence modeling for Free-Space Optical system," 17th International Conf. on Telecommn. 2010, pp. 487–492. https://doi.org/10.1109/ICTEL.2010.5478872
[30] T. A. Tsiftsis, H. G. Sandalidis, G. Karagiannidis, and M. Uysal, "Optical wireless links with diversity over strong atmospheric turbulence channels," IEEE Trans. Wireless Commn., vol. 8, no. 2, pp. 951–957, Feb. 2009 https://doi.org/10.1109/TWC.2009.071318

[31] Omar M. Hasan, "Performance of heterodyne differential phase-shift keying system over double Weibull free-space optical channel," J. Modrn Optics. Vol. 62, no. 11, pp. 869–876, 2015. https://doi.org/10.1080/09500340.2015.1027311
[32] L. C. Andrews, and R. L. Philips, "*I-K* distribution as a universal distribution model of laser beams in atmospheric turbulence," J. Opt. Soc. *A* 2, pp. 160–163, 1985. https://doi.org/10.1364/JOSAA.2.000160
[33] M. A. Al-Habash, L. C. Andrews, and R. L. Philips, "Mathematical model for irradiance probability density function of a laser beam propagating through turbulent media," Optical Engineering, vol. 40, pp. 1554–1563, Aug. 2001. https://doi.org/10.1117/1.1386641
[34] S. M. Flatté, C. Bracher, and G.-Yu Wang, ''Probability-density functions of irradiance for waves in atmospheric turbulence calculated by numerical simulations,'' J. Opt. Soc. Am. A11, 2080–2092, 1994. https://doi.org/10.1364/JOSAA.11.002080
[35] Peng Deng, Mohsen Kavehrad, Zhiwen Liu, Zhou Zhou, and Xiuhua Yuan, "Capacity of MIMO free space optical communications using multiple partially coherent beams propagation through non-Kolmogorov strong tutbulence," Opt. Express, vol. 21, no. 13, pp. 15213–15229, 2013. https://doi.org/10.1364/OE.21.015213

## 8 Author

**Prof. Omar Hasan (Bani Ahmad)** received his PhD and MSc degrees in Communication Engineering, and BSc degree in Electrical Engineering from New Mexico State University, USA, 1996, 1990 and 1987 respectively. He joined Princess Sumaya University for Technology (PSUT) in 1997, where he chaired the communications engineering department at PSUT during the period 2005–2010. Prof. Omar has worked in the area of turbo coding and optical wireless communications, and has worked in different projects at physical science laboratory, Las Cruces, USA, 1991–1992.

Article submitted 2022-06-28. Resubmitted 2022-08-05. Final acceptance 2022-08-10. Final version published as submitted by the authors.